Electronic Supplementary Material (ESI) for Dalton Transactions.
This journal is © The Royal Society of Chemistry 2016

Supporting information for

Ligand dependent topology and spontaneous resolution in high-spin cyano-bridged Ni_3W_2 clusters

Beata Nowicka, Mateusz Reczyński, Michał Rams, Tadeusz Wasiutyński, Wojciech Nitek, and Barbara Sieklucka

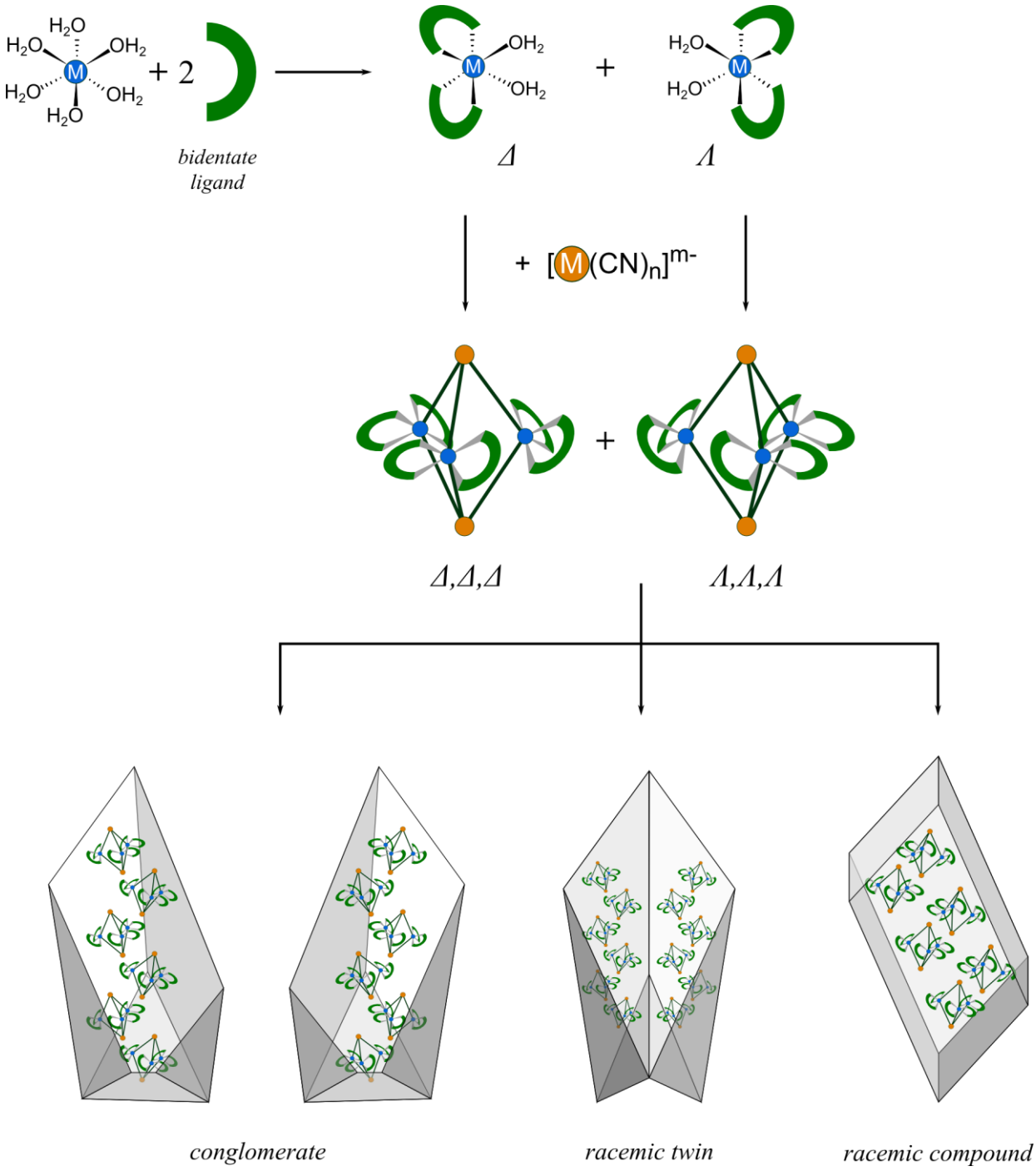

Scheme S1. Formation of chiral clusters of TBPY topology from bis-bidentate cationic precursor complexes and polycyanometallates.

Table S1. Selected bond angles (°) for **1Δ**, **1Λ** and **2**

	1Δ	**1Λ**		**2**
angles of bridging CN				
C11-N11-Ni1	169.4(7)	168.0(6)	C13-N13-Ni1	166.0(4)
C12-N12-Ni2	164.0(8)	162.5(7)	C14-N14-Ni2	159.4(4)
C13-N13-Ni3	167.5(7)	165.7(6)	C15-N15-Ni3	161.4(4)
C21-N21-Ni1	171.1(9)	172.8(7)	C23-N23-Ni1	160.6(3)
C22-N22-Ni2	169.1(9)	170.7(8)	C24-N24-Ni2	172.5(4)
C23-N23-Ni3	169.3(8)	170.4(7)		
angles at metal centres				
C11-W1-C12	75.4(3)	75.3(3)	C13-W1-C14	73.68(15)
C11-W1-C13	75.5(3)	75.2(3)	C13-W1-C15	139.13(17)
C12-W1-C13	75.0(3)	74.4(3)	C14-W1-C15	143.89(16)
C21-W2-C22	72.1(4)	72.7(3)	C23-W2-C24	74.93(16)
C21-W2-C23	88.5(3)	88.4(3)		
C22-W2-C23	73.7(4)	73.1(3)		
N11-Ni1-N21	91.2(3)	90.7(3)	N13-Ni1-N23	91.29(14)
N31-Ni1-N39	77.6(3)	77.8(3)	N31-Ni1-N44	79.96(14)
N47-Ni1-N55	78.3(3)	78.2(3)	N45-Ni1-N58	79.79(15)
N12-Ni2-N22	88.8(3)	89.7(3)	N14-Ni2-N24	92.25(15)
N63-Ni2-N71	76.4(3)	75.8(4)	N59-Ni2-N72	79.64(18)
N79-Ni2-N87	79.1(3)	78.4(3)	N73-Ni2-N86	79.48(17)
N13-Ni3-N23	91.3(3)	90.8(3)	N15-Ni3-O115	92.32(17)
N95-Ni3-N103	77.3(3)	76.9(3)	N87-Ni3-N100	79.28(16)
N111-Ni3-N119	77.1(3)	78.4(3)	N101-Ni3-N114	80.46(19)

Table S2. Selected distances (Å) and angles (°) between metal centres

	1Δ	**1Λ**		**2**
intra-cluster distances				
Ni1-W1	5.370	5.368	Ni1-W1	5.321
Ni1-W2	5.296	5.294	Ni1-W2	5.282
Ni2-W1	5.305	5.305	Ni2-W1	5.299
Ni2-W2	5.335	5.334	Ni2-W2	5.312
Ni3-W1	5.337	5.346	Ni3-W1	5.298
Ni3-W2	5.349	5.346		
Ni1-Ni2	6.259	6.271	Ni1-Ni2	6.829
Ni2-Ni3	6.365	6.366		
Ni3-Ni1	6.954	6.951		
W1-W2	7.520	7.518	W1-W2	8.067
intra-cluster angles				
W1-Ni1-W2	89.67	89.67	W1-Ni1-W2	99.07
W1-Ni2-W2	89.96	89.92	W1-Ni2-W2	98.96
W1-Ni3-W2	89.46	89.36		
Ni1-W1-Ni2	71.79	71.97	Ni1-W1-Ni2	80.03
Ni1-W1-Ni3	81.00	80.91	Ni1-W2-Ni2	80.26
Ni2-W1-Ni3	73.47	73.41	Ni1-W1-Ni3	147.70
Ni1-W2-Ni2	72.14	72.32	Ni2-W1-Ni3	127.64
Ni1-W2-Ni3	81.57	81.58		
Ni2-W2-Ni3	73.13	73.18		
Ni1-Ni2-Ni3	66.84	66.73		
Ni2-Ni3-Ni1	55.85	55.98		
Ni3-Ni1-Ni2	57.31	57.29		
inter-cluster distances				
W2-Ni3'	9.129	9.115	Ni2-Ni3'	8.896
W1-Ni1'	9.255	9.275	Ni1-Ni2'	9.013
Ni1-Ni3'	9.748	9.770	Ni1-Ni3'	9.189
Ni2-Ni1'	9.964	10.042	W1-Ni3'	9.402

Table S3. Continuous Shape Measure Parameters (SChM) calculated with SHAPE 2.1

compound	ion	SAPR-8	TDD-8	BTPR-8	JBTPR-8
1Δ	W1	0.335	1.676	1.438	2.078
	W2	2.772	0.551	1.611	2.422
1Λ	W1	0.364	1.541	1.418	2.013
	W2	2.831	0.591	1.639	2.438
2	W1	0.333	1.715	1.532	2.170
	W2	0.667	1.217	1.704	2.302

compound	**1Δ**			**1Λ**			**2**		
ion	Ni1	Ni2	Ni3	Ni1	Ni2	Ni3	Ni3	Ni4	Ni5
OC-6	0.830	0.894	0.762	0.810	0.989	0.718	0.564	0.642	0.611

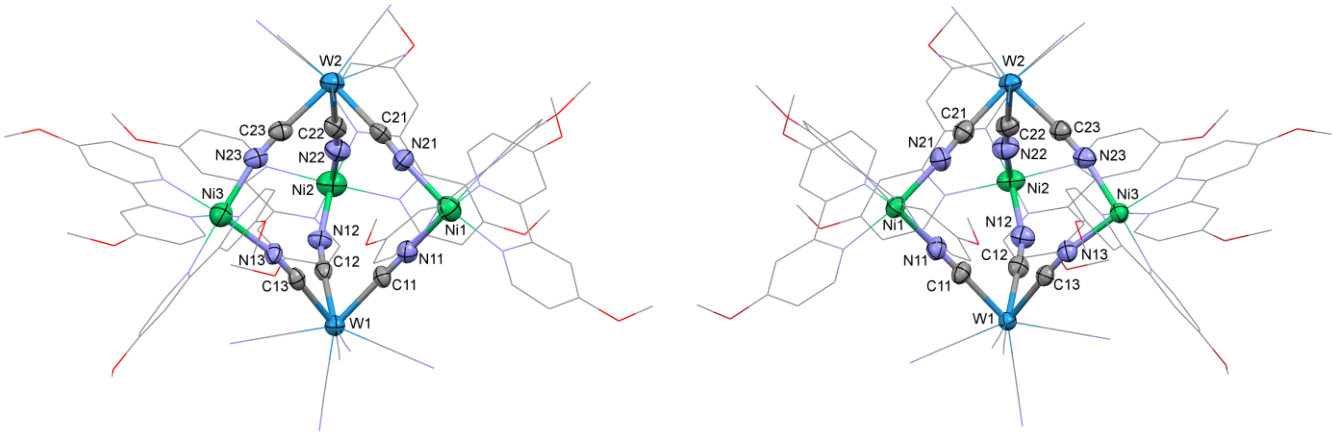

Figure S1. The structure of **1Δ** (left) and **1Λ** (right) with principal atoms numbering; hydrogen atoms and water molecules omitted for clarity; terminal ligands represented by sticks: C - grey, N - blue, O - red.

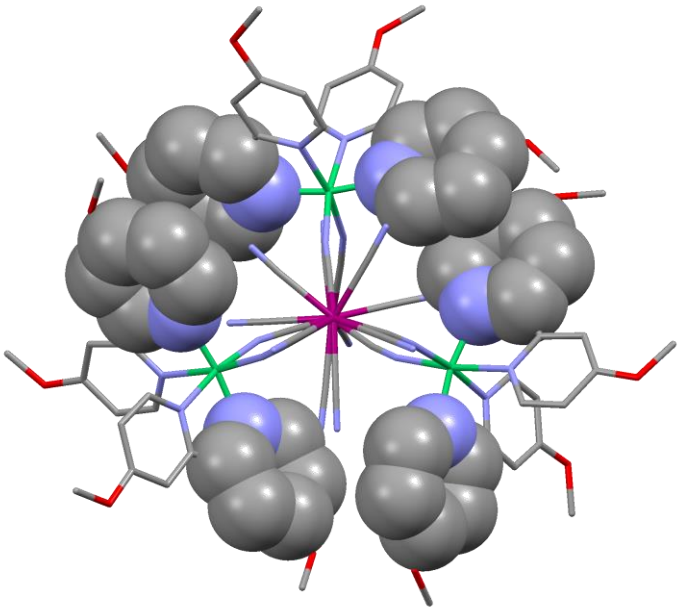

Figure S2. Intra-cluster π-π interactions in **1Λ**.

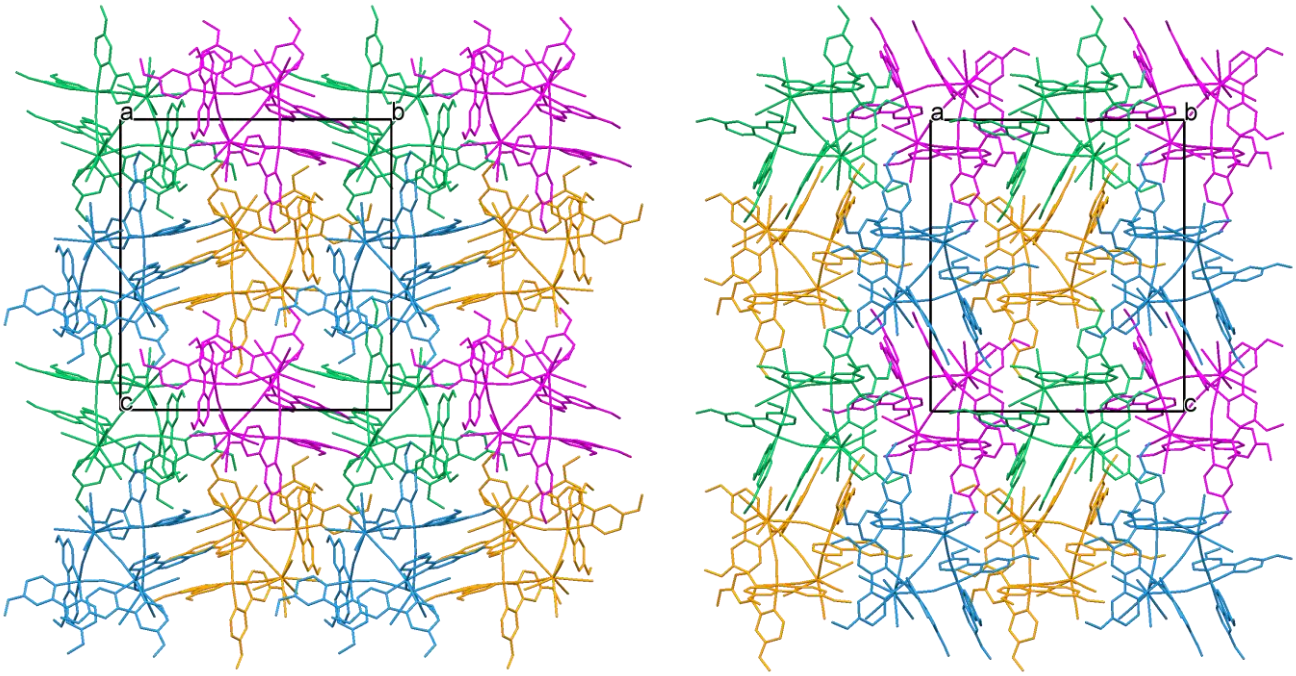

Figure S3. Packing diagram of **1Λ** - view along *a* (left) and *b* (right) axis; clusters at different positions in the unit cell marked with different colours; water molecules omitted for clarity.

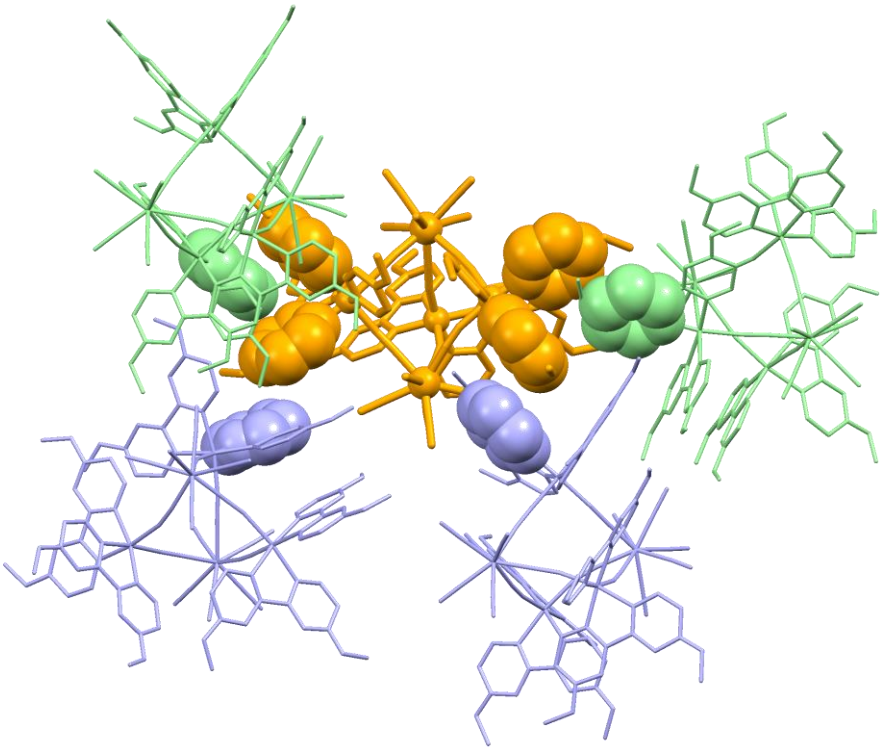

Figure S4. Inter-cluster π-π interactions in **1Λ**. Four out of six neighbouring clusters are shown for the cluster in the centre (yellow).

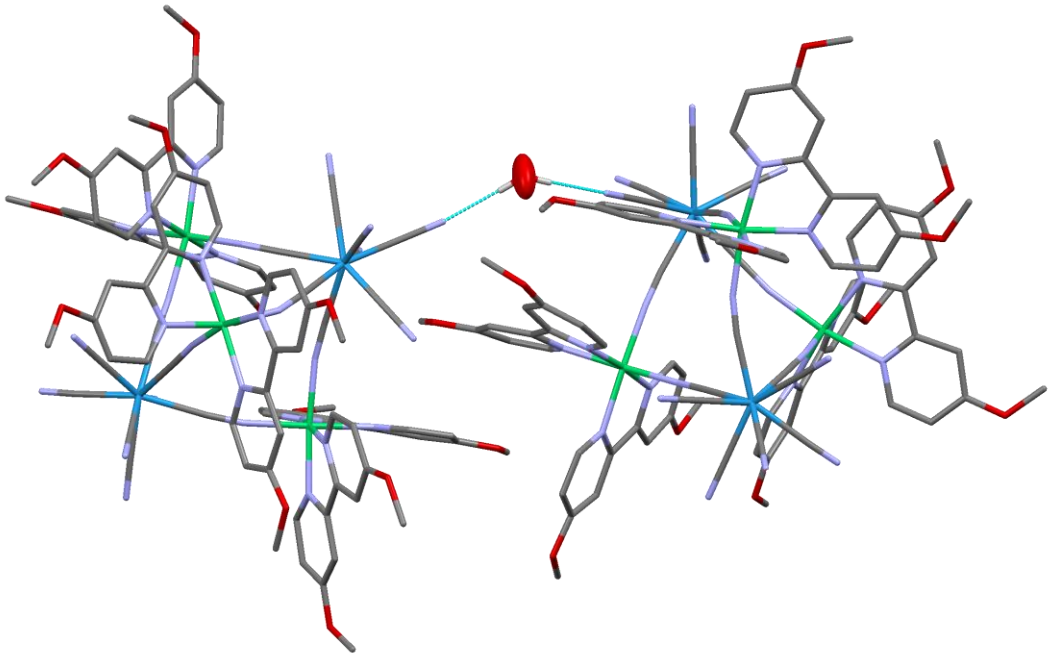

Figure S5. Localised water molecule and hydrogen bonds in the structure of **1Λ**.

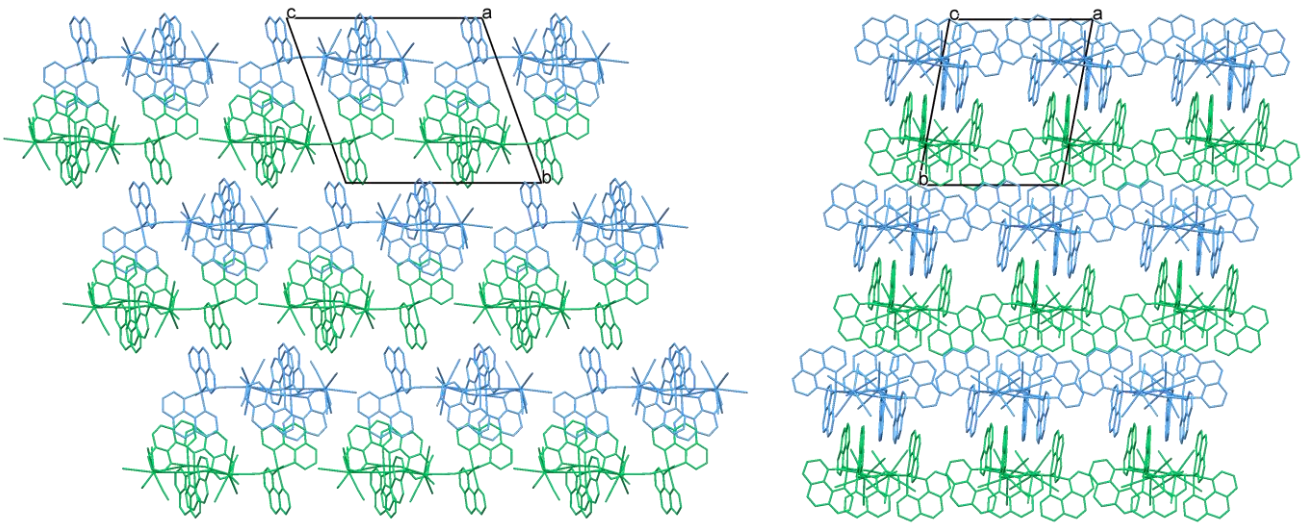

Figure S6. Packing diagram of **2** - view along the *a* (left) and *c* (right) axis with visible layers of clusters of ΔΔΔ (blue) and ΛΛΛ (green) configuration; water molecules omitted for clarity.

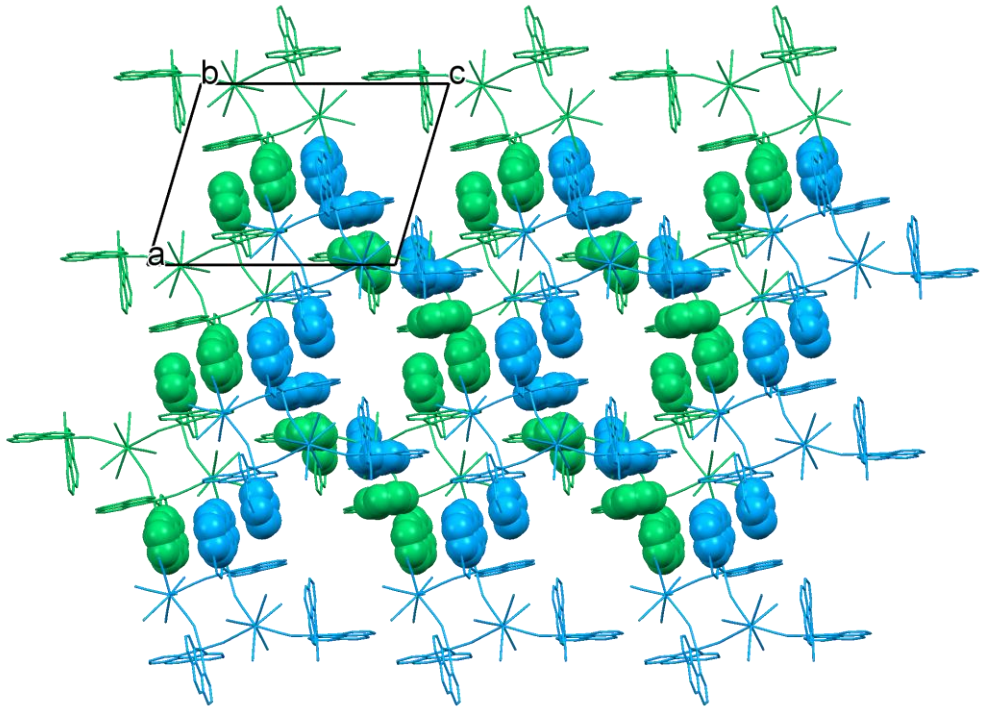

Figure S7. Inter-cluster π-π interactions in **2** - view along *b* axis; blue - ΔΔΔ, green - ΛΛΛ clusters.

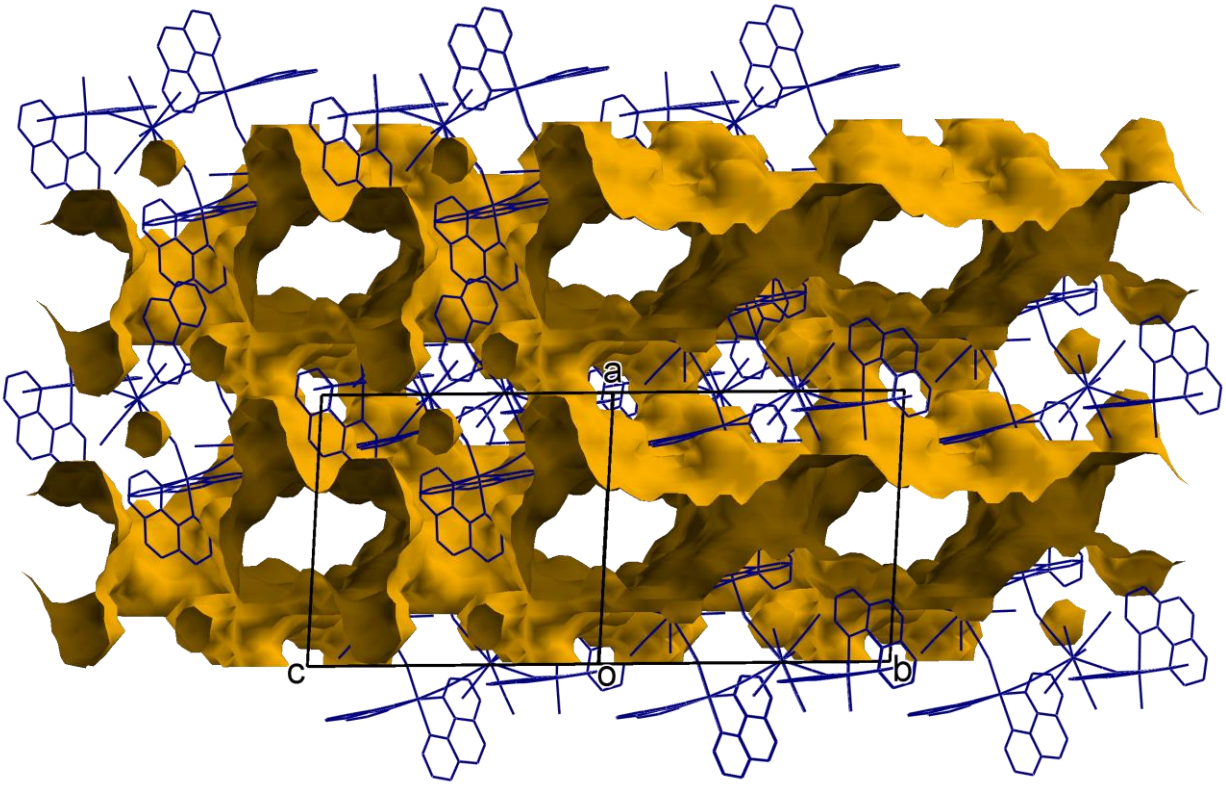

Figure S8. Channels in the structure of **2** - view along [011] direction.

Terms for magnetization M_5 and magnetic susceptibility χ_5 of individual clusters used in the fitting procedure:

$$M_5 = RT \frac{\partial \ln z}{\partial H} \quad (1)$$

$$\chi_5 = \frac{\partial M_5}{\partial H} \quad (2)$$

where

$$z = \sum_i \exp \frac{-E_i}{k_B T}$$

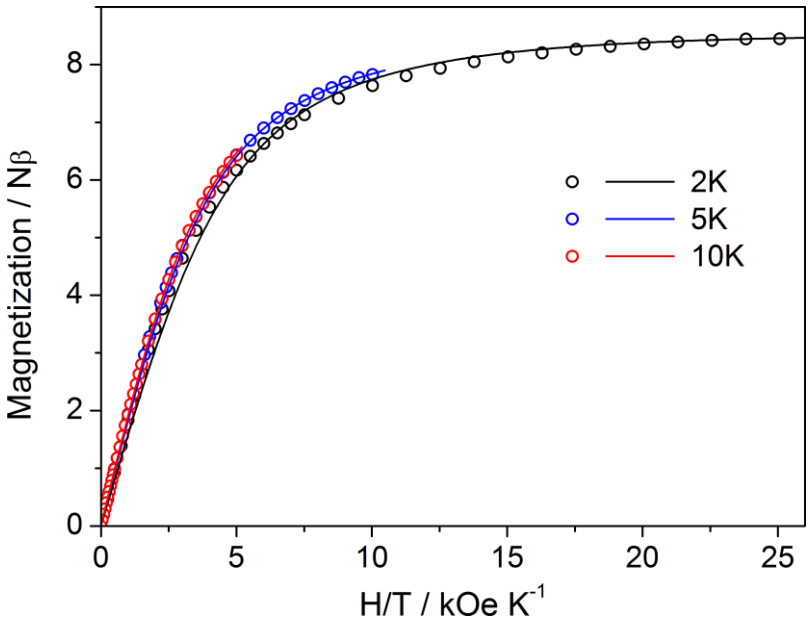

Figure S9. Magnetisation *vs. H/T* for measurements at 2, 5 and 10 K for **1**. Solid lines represent curves calculated on the basis of the applied model.

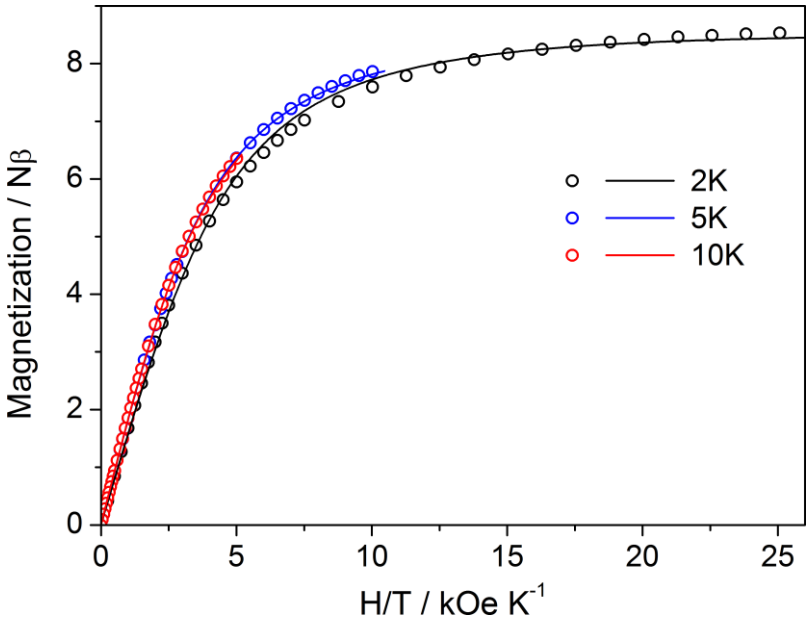

Figure S10. Magnetisation *vs. H/T* for measurements at 2, 5 and 10 K for **2**. Solid lines represent curves calculated on the basis of the applied model.

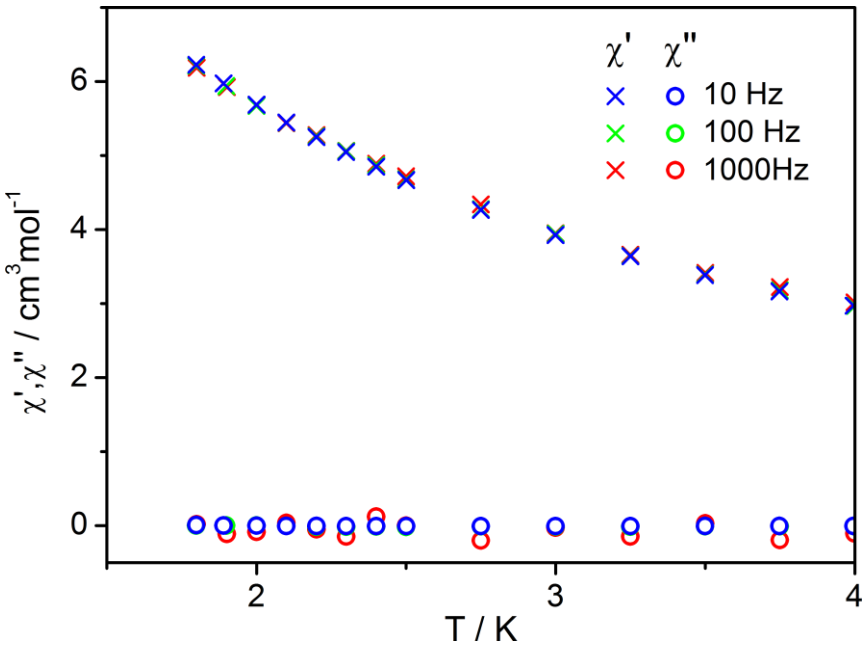

Figure S11. AC magnetic susceptibility for **1** at 0 DC field; application of 1 kOe DC field has no influence on the AC susceptibility.

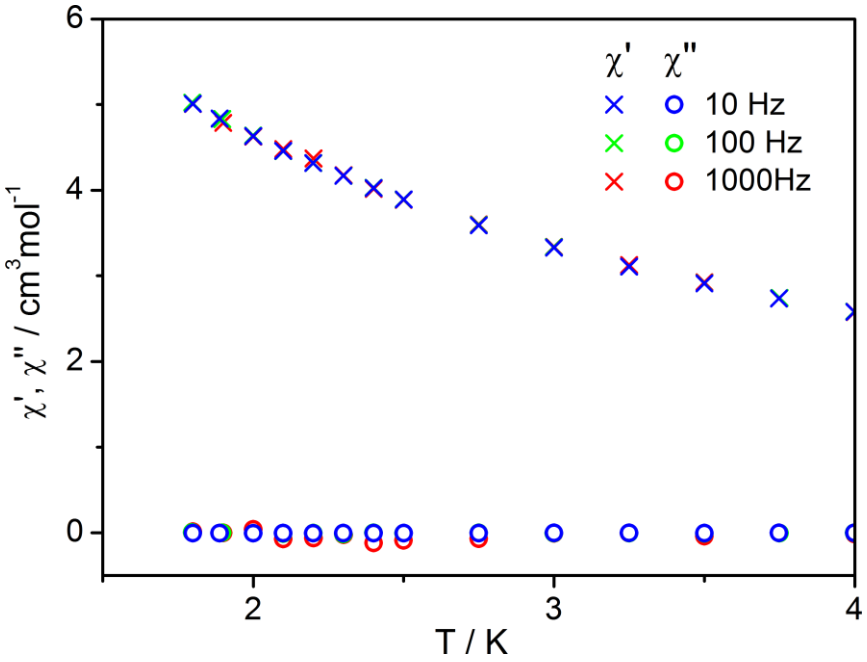

Figure S12. AC magnetic susceptibility for **2** at 0 DC field; application of 1 kOe DC field has no influence on the AC susceptibility.

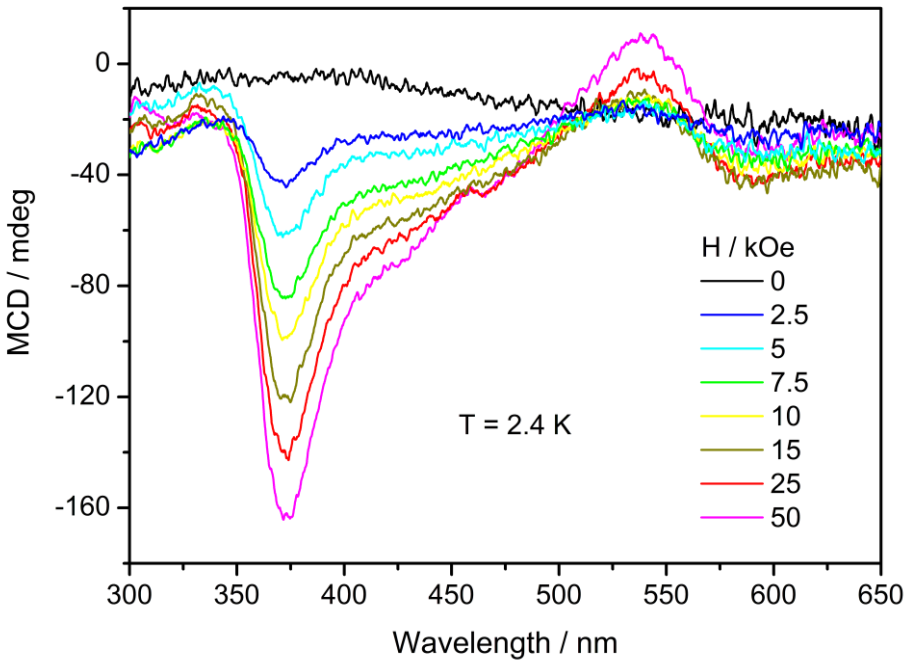

Figure S13. Magnetic circular dichroism spectra for **1** measured at 2.4 K with different applied field.

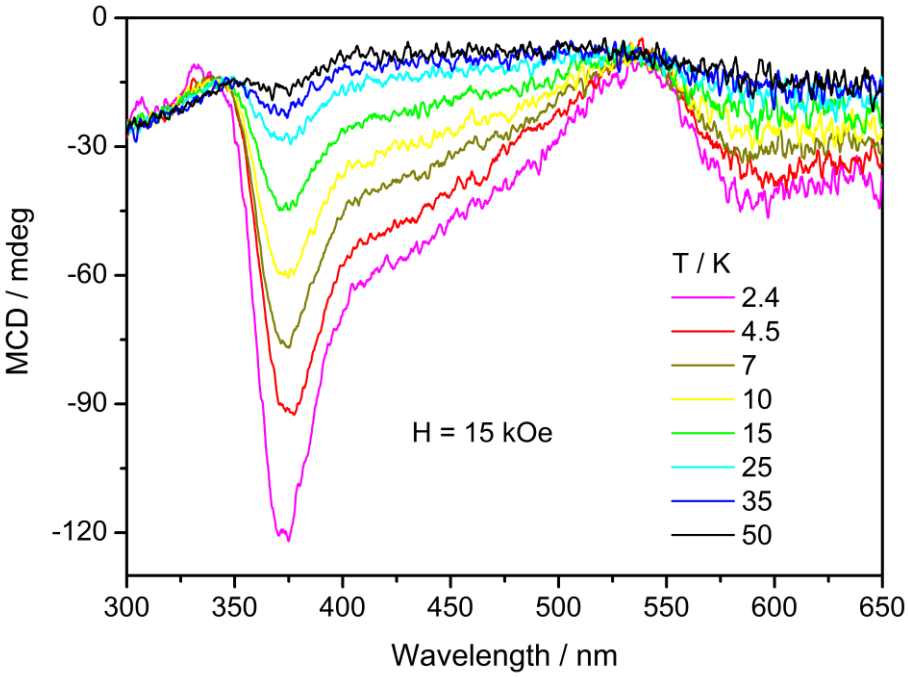

Figure S14. Magnetic circular dichroism spectra for **1** measured for different temperatures at the applied field of 15 kOe.